More Resilient Wall Building Structures

Lead Investigator:

Professor Santiago Pujol, University of Canterbury

Research Team:

Associate Professor Rick Henry, University of Auckland

Charles Kerby, PhD Candidate, University of Canterbury

May 31st, 2024

Acknowledgements

The research team would like to acknowledge EQC Toka Tū Ake (now called the Natural Hazards Commission Toka Tū Ake, as of 1 July 2024) for awarding a 2022 Biennial Grant as the primary funding source for this project.

Additional funding was provided by Te Hiranga Rū QuakeCoRE.

Experimental work was completed in the University of Canterbury's Structural Engineering Laboratory.

Construction materials were provided in part by Complete Reinforcing - a business division of Euro Corporation, Firth Concrete, and Sika New Zealand Limited. Material testing was completed in part by Holmes Solutions.

Executive Summary

This project addressed a gap in knowledge regarding the seismic resilience of multi-storey buildings in Aotearoa New Zealand. Reinforced concrete structural walls are one of the most common and effective means of protecting buildings against earthquakes. To be effective, structural walls need to be 1) proportioned appropriately for the building, 2) constructed on a sturdy foundation, and 3) soundly connected to that foundation. But currently New Zealand standards allow a reinforcement configuration for connecting reinforced concrete structural walls to their foundations called "staggered lap splices". The configuration is not permitted in concrete walls designed to sustain large lateral deformations during earthquakes in highly seismic regions of other countries such as the USA and Japan. Staggered lap splices were thought to be an improvement over other reinforcement configurations (e.g. non-staggered lap splices) that were already known to be vulnerable to losses of lateral load resistance at relatively small lateral deformations during earthquakes compared to design expectations. New Zealand design practice does not permit non-staggered laps near critical sections of RC walls expected to sustain large lateral deformations, and the staggering laps was perceived as a way to improve the deformability of walls with lap splices. But staggered lap splices had never been experimentally tested in walls to confirm improved resilience. The experiments completed in this project were the first full-scale tests of reinforced concrete structural walls with staggered lap splices in the world.

Six reinforced concrete structural walls, each approximately eight meters tall, were tested at the University of Canterbury's Structural Engineering Laboratory. Four walls had staggered lap splices designed to be compliant with the current version of New Zealand's concrete structures standard. One wall had non-staggered lap splices, which is not currently permitted in New Zealand design practice. The final wall tested an alternative method of connecting walls to their foundations, namely the mechanical coupling of vertical reinforcement. Experiments recorded how damage might accumulate during an earthquake, how walls deformed under intense loading, and the ultimate strength and deformability of the walls.

Walls with staggered lap splices were observed to be as or even more vulnerable to losses of lateral load resistance at lateral deformations lower than expected in design than walls with non-staggered lap splices are. The experimental results suggest the permissibility of including "staggered lap splices" in the design practice of reinforced concrete structural walls expected to sustain large lateral deflections during earthquakes should be comprehensively reviewed.

Technical Abstract

Lap splices, in both their detailing and location, are critical to the performance of reinforced concrete (RC) walls. Failures of in-situ RC walls associated with lap splices were most recently recorded after earthquakes in Chile (2010), New Zealand (2011), Taiwan (2016), and Turkey (2023). But collapses attributed to lap-splice failures go as far back as the Alaska Earthquake of 1964 [1] in which a control tower and an apartment building were reported to have had short non-staggered lap splices in wall vertical reinforcement, among other deficiencies.

Collapse of the Four-Seasons Apartment Building in Anchorage, Alaska [1]

Previous experiments confirmed that RC wall deformability can be reduced not only by bond failure of lap splices, but also by concentrations of strain near the ends of non-staggered lap splices. As a consequence, lap splices of longitudinal reinforcement in boundary elements of structural RC walls designed to sustain large ductility demands now must be either staggered (as in New Zealand) or located away from sections where reinforcement may yield (as in the USA). While the purpose of both design restrictions is to improve wall deformability by reducing the concentration of strains that occurs near the ends of lap splices, no explicit study had previously been made to quantify the deformability of RC walls with staggered lap splices. An experimental program consisting of six full-scale, cantilever RC walls with rectangular and symmetric cross sections was performed. Wall height-to-length aspect ratio was 3.2 and shear span was 6.45 meters. Four walls had lap splices of longitudinal reinforcement located near the section of maximum moment, staggered by half the lap length. One wall had non-staggered lap splices. The remaining wall had mechanical couplers splicing longitudinal bars instead of lap splices. Results showed that inelastic strains concentrated near the ends of all lap splices, whether staggered or not. The drift ratio (lateral deflection at line of action of applied lateral load divided by the shear span) at first failure was the lowest in the four walls with staggered lap splices. The worst performing wall had staggered lap splices, and a drift ratio at first failure of just 1.0%. Where splicing method was the primary variable, a wall with staggered lap splices had a drift ratio at first failure of 1.7%, approximately 1.3 times smaller than a nominally equivalent wall with non-staggered lap splices and 2.0 times smaller than a nominally equivalent wall with mechanical couplers. Results suggest walls with staggered lap splices near sections where reinforcement yields are at least as vulnerable to failure during earthquakes as walls with non-staggered lap splices.

Keywords

Earthquake, Resilient Buildings, Reinforced Concrete, Structural Wall, Lap Splice

Introduction

The overlapping of steel reinforcement bars, called a lap splice, is a traditional and convenient method to splice bars in reinforced concrete (RC). Lap splices transfer forces between spliced reinforcing bars via the surrounding concrete. The splice length (L_s) is the length of the overlap between spliced bars. The relative locations of adjacent lap splice ends define splice "stagger" (Figure 1). Lap splices are non-staggered if adjacent splice ends are aligned and are staggered when adjacent splice ends are not aligned. Splice stagger is defined by a stagger distance, commonly equal to $0.5 * L_s$ (as shown in Figure 1), $1.0 * L_s$, or $1.3 * L_s$.

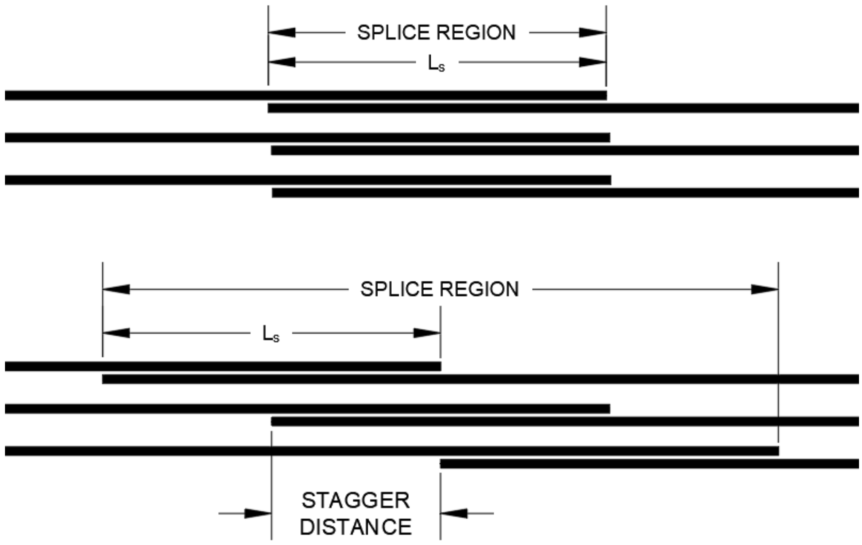

Figure 1: Illustration of non-staggered (top) and staggered (bottom) lap splices

Damage associated with lap splices of longitudinal reinforcement has been observed after major earthquakes, including in buildings recently constructed. In the last two decades, failures of RC walls caused at least in part by the presence of lap splices were recorded after 2010 Chile (Maule) (Figure 2) [2], 2011 New Zealand (Canterbury) [3], 2016 Taiwan (Meinong) [4] and 2023 Turkey-Syria [5] earthquakes.

During the February, 2011 Christchurch earthquake the PGC building collapsed when the top four stories of the building split from the ground storey and overturned (Figure 3). The sequence of failures leading to total collapse was likely instigated by tensile failures of reinforcement in the structural core walls occurring at strain concentrations caused by low reinforcement ratios in the walls [3] and/or the presence of non-staggered lap splices of vertical reinforcement near the failure section.

These field observations led to extensive full-scale testing of the strength and deformability of RC structural walls with non-staggered lap splices near sections where reinforcement yields. A total of 20 walls with non-staggered lap splices had been tested before this investigation ([6] [7] [8] [9] [10] [11] [12] [13] [14] [15]). The consensus reached was that 1) lap splice failure can be the controlling failure mode of RC structural walls and 2) inelastic strains develop only outside of non-staggered lap splice regions, reducing deformability relative to walls with continuous reinforcement. No experiments were conducted to study whether the same conclusions apply to walls with staggered lap splices.

There has been recent international reaction to field observations and experimental studies of lap splice failures in RC walls. Since 2019, building standards such as ACI 318-19 in the USA [16] have not permitted the placement of lap splices in boundary elements and near critical sections of structural walls. In contrast, the current New Zealand RC Standard, NZS 3101:2006 (A3) [17], states that:

> **11.4.8.1** *Splicing of flexural tension reinforcement*
> *The splicing of the principal vertical flexural tension reinforcement in the ductile detailing length in ductile walls shall be avoided if possible. Not more than one-third in ductile plastic regions, and one-half for limited ductile plastic regions of such reinforcement shall be spliced at the same location where yielding can occur.*

To the knowledge of the authors, when NZS 3101 was amended to continue to allow staggered lap splices near critical sections in walls designed to sustain large ductility demands, the decision was made without supporting experimental evidence.

Figure 2: Collapse of the Alto Rio building after the 2010 Chile (Maule) earthquake (reproduced from [2])

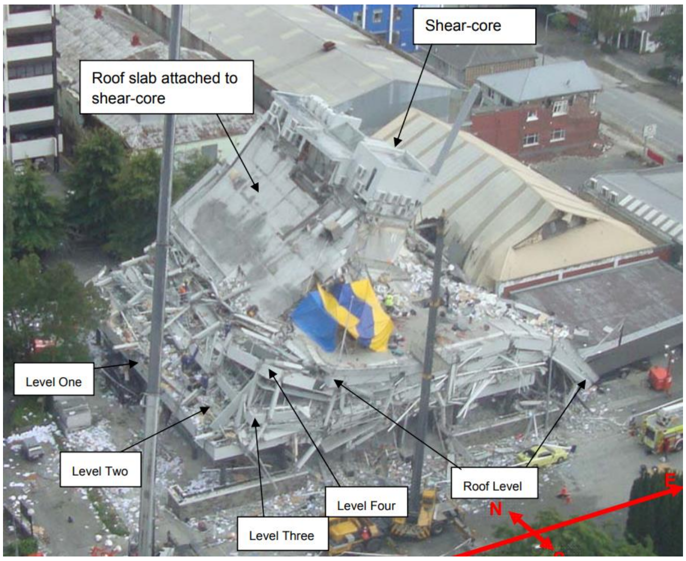

Figure 3: Collapse of the PGC building after the 2011 New Zealand (Canterbury) earthquake sequence (reproduced from [3])

The experiments described in this report included the first tests of full-scale RC structural walls with staggered lap splices. Walls were tested as cantilevers loaded at a single location above foundations fastened to a 'strong' reaction floor. The height-to-length aspect ratio of the test walls was approximately 3.2, and the conclusions of this report should be expected to apply to walls with height-to-length aspect ratios greater than 2.0. Six walls were tested: four with staggered lap splices, one with non-staggered lap splices, and one with mechanical couplers.

Discussion

The seismic resilience of a structural wall is best defined by the wall's deformability. In this report, deformability of walls is discussed in terms of the drift ratio at the first structural failure, where drift ratio is the lateral displacement at the top of the wall divided by the height of the wall. This definition of deformability is chosen as the first failure in a structural wall corresponds to 1) the development of damage that will require extensive repairs and 2) the first change in wall seismic response causing an increase in wall vulnerability to future earthquakes [18] [19].[1] Experimental methodology and results are presented in Appendices A and B.

In Appendix B, Table 5 lists the drift ratio at first failure of each of the six walls tested. Test Wall WC, having mechanical couplers instead of lap splices, achieved the highest drift ratio before failure (3.5%). The drift ratio at first failure of Wall WC was 1.5 times larger than that of the best performing wall with lap splices (Wall W4 with non-staggered lap splices reached a drift ratio of 2.3%) and was 3.5 times larger than the worst (Wall W1 with staggered lap splices reached a drift ratio of 1.0%).

All the walls with lap splices had bond failures along lap splices. In all instances, bond failure caused an abrupt drop in lateral resistance consistent with the total loss of tensile stresses in the affected bars. In static displacement-controlled tests such as those described here, such an abrupt drop in resistance does not compromise structural stability. Nevertheless, similar failures in elements resisting gravity loads and dynamic demands can compromise stability. Consider also that NZS 1170.5 allows a maximum storey drift ratio of 2.5%, which corresponds to a roof drift ratio of nearly 2%, on average. The drift capacities achieved by the five test walls with lap splices either fall below this value or leave very little margin of safety against errors in predictions of the demands associated with future ground motions. Given the overwhelming uncertainties in ground motion prediction, the deformation capacities of structural walls should exceed expected demands by ample margins. It is worth reiterating that all the test walls were detailed to meet current seismic design standards [17].

Inelastic strain distributions

The deformation capacity of an in-situ RC structural wall depends primarily on the distribution of inelastic strains within the wall. Current New Zealand design [17] and assessment [20] standards are based on the assumption that well designed walls can develop inelastic strains over a large region near the section of maximum moment. The comparison of inelastic strain distributions is most easily made by comparing measurements of surface deformations obtained from Test Walls W3 (with staggered lap splices), W4 (with non-staggered lap splices), and WC (with mechanical couplers to splice bars). The only variable (beyond minor differences in material properties) differentiating these three test walls is the method of splicing reinforcement. Measured concrete surface strains are plotted as a contour map in Figure 4. The measurements used to create the three strain maps were taken at the same drift ratio (1.5%) and prior to failure in any of the test walls.

At the same drift ratio, the largest inelastic strains occurred at the base of W3 (Figure 4a). The staggered lap splices of W3 did not disperse the concentrations of inelastic strains known to occur in walls with non-staggered lap splices such as W4 (Figure 4b). On the contrary, concentration of strains seems to be more pronounced for the wall with staggered lap splices (W3) than for the wall with non-staggered lap splices (W4). The extended height of the staggered splice region (as defined in Figure 1) allowed no plasticity to

[1] Another common definition of deformability is "the drift ratio at which 20% of the resistance to lateral load has been lost". This definition is not used in this report as the "20% loss of resistance" was arbitrarily chosen, and extensive repairs to structural walls could be required well before that limit is reached.

develop anywhere above the base of the wall. In contrast, the shorter length of the non-staggered splice region in Wall W4 led to some plasticity at an elevation of approximately 1-meter (Figure 4b). A distribution of inelastic strains that is more consistent with what is expected in conventional wall design was observed only in the test wall without lap splices (Wall WC, Figure 4c). All three test walls of Figure 4 had over twice the quantity of transverse reinforcement confining the boundary elements as is required for "ductile" detailing in NZS 3101, but neither wall with lap splices recreated a desirable strain distribution.

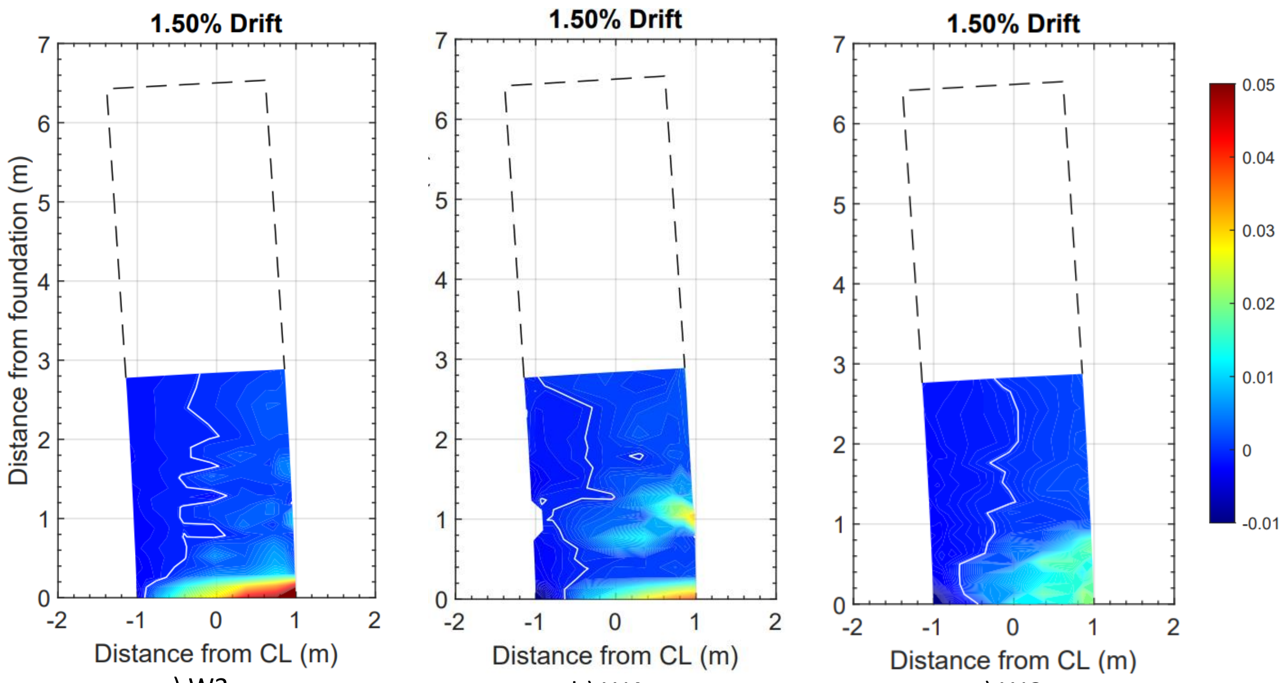

Figure 4: Longitudinal strain maps of W3 (staggered splices), W4 (non-staggered splices), and WC (mechanical couplers) from measurements taken at 1.50% drift

The strain maps of Figure 4 are likely to have been sensitive to the length of the splice region, the gauge length used to define strains, and the moment gradient. Nevertheless, it is remarkable that at a drift ratio of 1.5%, the peak strain observed at the base of the test wall was approximately 2.5 times larger in W3 than in WC. This large discrepancy suggests that conventional methods to quantify the deformability of a wall based on sectional indices such as strain or curvature are not useful in the case of walls with lap splices. Their applicability is limited by both the differences in the heights of the regions that can accommodate plastic deformations and the propensity of the lap splice to fail in bond.

The observed strain distributions illustrate that walls with staggered lap splices can be even more susceptible to failure during earthquakes than walls with non-staggered lap splices, which were already known to be vulnerable to loss of resistance to lateral loads at relatively low ductility demands. It follows that all walls with lap splices near sections where reinforcement yields, regardless of lap splice stagger, have reduced deformation capacity relative to walls with no lap splices.

Comparison to current design expectations for deformability

The current iteration of the New Zealand RC standard [17] defines material strain limits within "plastic-hinge" regions of RC walls. Within the bounds of this experimental setting, the material strain limits and associated rotation limits of NZS 3101 can be reasonably equated to a "design drift capacity" for each wall[2].

[2] A limiting plastic hinge rotation, when multiplied by the shear span, approximates a limiting lateral deflection for the experimental test setup used in this report (cantilever walls laterally loaded along a single line of action).

Design limits are meant to be conservative, and engineers often assume that walls meeting current code requirements will be able to at least achieve the calculated capacity without suffering any failure.

Calculations of design drift capacities are based on estimated inelastic strains distributed over a large region (called the “plastic hinge”). These design assumptions are illustrated in Figure 4c, where inelastic strains in Wall WC are distributed over a large region near the base of the wall. But the same assumption does not apply to walls with lap splices, as shown in Figure 4a and 4b where strains concentrated only near lap splice ends. The discrepancy between the assumptions made in design calculations and what has been observed in tests of walls with lap splices can result in non-conservative design of RC structural walls.

The design drift capacity for the geometry and reinforcement detailing of the six test walls was calculated according to the current NZ RC design standard [17] to be approximately 2.8% (see Appendix C for methodology). The calculation of this design drift capacity assumes that an engineer would first confirm that each wall meets the minimum requirements for “ductile detailing” (which is true for all six walls) and next would assume that any wall meeting this detailing standard can achieve at least the maximum allowable design deformation capacity prescribed in [17], as would be required for a conservative design. The design drift capacity of 2.8% is compared to the experimental drift at first failure for each of the six walls in Figure 5.

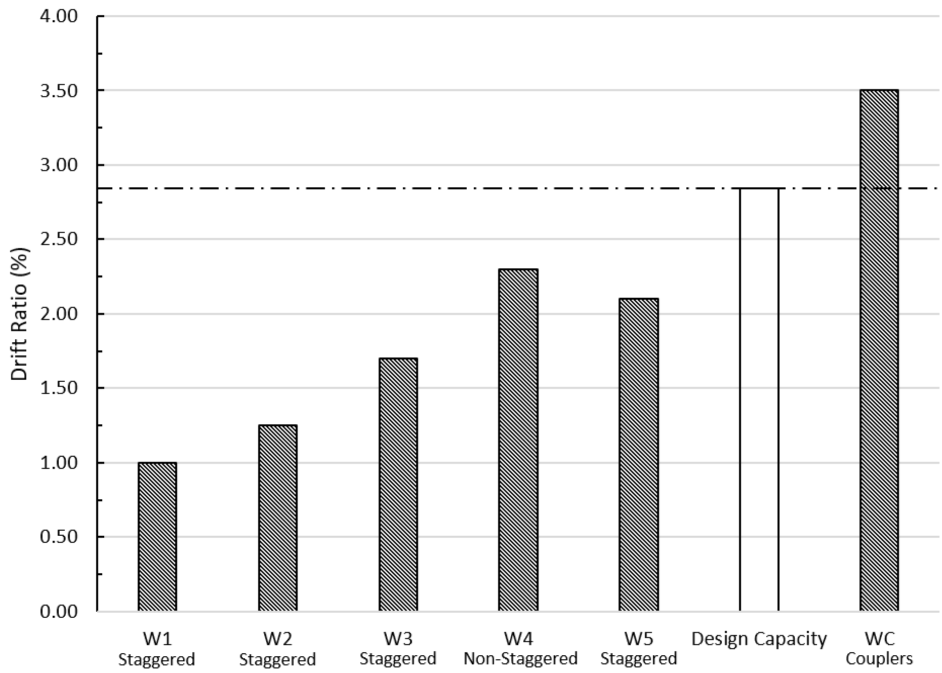

Figure 5: Drift ratio at first failure as calculated in design according to NZS 3101:2006 (A3) [17] and as measured in experiments.

Only Wall WC, with mechanical couplers instead of lap splices, exceeded the design drift capacity. The design drift capacity was approximately 0.80 times as large as the drift at first failure of Wall WC, which is on par with the margins assumed to be present in conservative design methods. In contrast, none of the walls with lap splices achieved the design drift capacity. The 2.8% design drift limit was approximately 1.25 times larger than the drift ratio at first failure of the best performing wall with lap splices (Wall W4) and approximately 2.8 times larger than the worst performing wall with lap splices (Wall W1).

Figure 5 illustrates that all five walls with lap splices could be non-conservatively designed under the current design standard requirements for walls expected to sustain large ductility demands. Employing current design practices, walls with lap splices may not be able to sustain a design-level earthquake without suffering structural failure if expected to achieve the full deformation capacity of a wall with a “ductile” plastic hinge according to NZS 3101. That none of the walls with lap splices reached the estimated design drift capacity supports that 1) whether or not lap splices should be permitted near critical sections of RC walls designed to sustain large ductility demands should be reconsidered and 2) the deformation capacity of walls with lap splices designed under current or past iterations of the New Zealand RC standard should be reassessed[3].

More detailed calculations of design drift limits for each wall based on deformation mechanics, estimated strain capacities of the lap splices, and the varying assumptions possible in design are explained in detail in Appendix C and support the same conclusions as Figure 5.

[3] The influence of lap splices on the deformation capacity of existing reinforced concrete walls is further discussed in publication (1) / reference [23].

Conclusions

This report summarized the results from six full-scale tests of reinforced concrete structural walls, completed at the University of Canterbury. Four of the walls (W1, W2, W3, and W5) had staggered lap splices of longitudinal reinforcement located near the base. One wall (W4) had non-staggered lap splices near the base, a reinforcement detail not permitted in New Zealand in the design of concrete walls expected to sustain large ductility demands. The final wall (WC) used mechanical couplers to connect reinforcement instead of lap splices and acted as a reference for what desired performance looked like within the bounds of the experimental program. The results support the following conclusion:

Compared to walls without lap splices, walls with lap splices near sections where reinforcement yields have reduced deformation capacities. This conclusion applies equally to walls with staggered lap splices and walls with non-staggered lap splices.

Staggering lap splices near sections where reinforcement yields did not prevent concentrations of strain at splice ends. The common design assumption that inelastic strains would distribute over a large region near the wall base was applicable only to the test wall with no lap splices. The deformability of walls with lap splices was reduced in two ways. First, the presence of lap splices caused concentrations of strain that were fundamentally different than strain distributions commonly assumed in design. Second, lap splices limited the peak strains that were achieved in the vertical reinforcement. The two mentioned effects (i.e. concentration of deformations and reductions in maximum usable strains) were observed to cause decreases in wall deformability of up to 70% relative to a wall with no lap splices.

It is recommended that lap splices, staggered or non-staggered, should not be permitted in regions of RC walls expected to sustain large inelastic strain demands during earthquakes. Similar language as is employed in ACI318-19 [16] to exclude lap splices from regions of “special” structural walls should be considered by an advisory group to inform revisions to NZS 3101 [17].

Future Work

The most pressing issue regarding the seismic vulnerability of RC walls with lap splices is the question of how to retrofit a wall with lap splices to improve deformation capacity. Of the 20 experiments of walls with non-staggered lap splices that have been performed, only one study explored retrofit solutions (namely concrete jacketing and carbon fibre wrapping of non-staggered lap splices) [7]. The existing building stock of New Zealand should be reassessed to determine which buildings have RC walls vulnerable to failure because of lap splices, and retrofits will likely be required for many of the walls under review. Future retrofit experiments must consider the real-world viability of proposed retrofits, as regions of RC structural walls requiring retrofitting may be hard to access or may span multiple stories in high-rise buildings.

Secondly, the mechanics of walls with staggered lap splices requires further experimental study. While four walls with staggered lap splices and two reference walls have formed a strong experimental foundation, more tests should be performed to expand the scope of this report. Parameters to consider include alternate splice lengths, stagger distances and patterns, and bond conditions.

A 6-month extension to this project (end date of December 2024) will convene an industry advisory group to consider any necessary amendments to relevant New Zealand design (NZS 3101) and assessment (C5) standards to reflect the conclusions of this report. The group clearly communicate proposed changes to standards to practitioners with design advisory notes and the assistance from relevant structural engineering societies (e.g. SESOC and NZSEE). The advisory group will also identify retrofit techniques that may need further study to address the vulnerabilities identified within the project scope.

Publications and Communications

Media

Research may have major impact on concrete wall construction (2023). Toka Tu Ake EQC Media Release.
https://www.eqc.govt.nz/news/research-may-have-major-impact-on-concrete-wall-construction/

Amendments to New Zealand Standards

C5-1A: Part C - Detailed Seismic Assessment of Concrete Buildings C5-1A.
Amendment proposed to Equation C5.42.

Publications

(1) Pollalis, W., Kerby, C., & Pujol, S. (2024). *On Estimating the Drift Capacity of Reinforced Concrete Walls with Lap Splices at their Bases*. Bulletin of Earthquake Engineering. https://doi.org/10.1007/s10518-024-01944-7 https://link.springer.com/article/10.1007/s10518-024-01944-7

(2) Kerby, C., S. Pujol, and R. Henry. (2024). *RC Structural Walls with Staggered Lap Splices*. 18th World Conference on Earthquake Engineering 2024. Milan, Italy.

(3) Kerby, C., S. Pujol, and R. Henry. (2023). *Experimental Study of Staggered Lap Splices in RC Structural Walls*. Concrete NZ Conference 2023. Paper 22. Hamilton, NZ.

(4) Kerby, C., S. Pujol, and R. Henry. (2023) *Deformability of lap splices in RC strucutral walls*. NZSEE Conference 2023. Paper 0036. Auckalnd, NZ.

Contributions to PhD research programmes

The experiments described in this report make up the primary contribution towards the PhD research of Charles Kerby at the University of Canterbury.

References

1. USGS and W. Hansen, *Efects of the earthquake of March 27, 1964 at Anchorage, Alaska.* United States Geological Survey Prof. Paper 542-A, 1965.
2. Song, C., S. Pujol, and A. Lepage, *The collapse of the Alto Río building during the 27 February 2010 Maule, Chile, earthquake.* Earthquake Spectra, 2012. **28**: p. S301-S334.
3. Beca, *Investigation into the Collapse of the Pyne Gould Corporation Building on 22nd February 2011*. 2011, Beca Carter Hollings & Ferner Ltd. Department of Building and Housing, Wellington.
4. NCREE and Purdue, *2016 taiwan (meinong) earthquake*. 2016: https://datacenterhub.org/deedsdv/publications/view/534.
5. Pujol, S., et al., *Quantitative evaluation of the damage to RC buildings caused by the 2023 southeast Turkey earthquake sequence.* Earthquake Spectra, 2024. **40**(1): p. 505-530.
6. Aaleti, S., et al., *Cyclic response of reinforced concrete walls with different anchorage details: Experimental investigation.* Journal of Structural Engineering, 2013. **139**(7): p. 1181-1191.
7. Paterson, J. and D. Mitchell, *Seismic retrofit of shear walls with headed bars and carbon fiber wrap.* Journal of Structural Engineering, 2003. **129**(5): p. 606-614.
8. Elnady, E.M.M., *Seismic rehabilitation of RC structural walls*. 2008, McMaster University.
9. Bimschas, M., *Displacement based seismic assessment of existing bridges in regions of moderate seismicity*. 2010, ETH Zurich.
10. Hannewald, P., M. Bimschas, and A. Dazio, *Quasi-static cyclic tests on RC bridge piers with detailing deficiencies.* IBK Bericht, 2013. **352**.
11. Layssi, H. and D. Mitchell. *Experiments on seismic retrofit and repair of reinforced concrete shear walls*. in *Proceedings of the 6th International Conference on FRP Composites in Civil Engineering (CICE)*. 2012.
12. Birely, A.C., *Seismic performance of slender reinforced concrete structural walls*. 2012, University of Washington.
13. Villalobos Fernandez, E.J., *Seismic response of structural walls with geometric and reinforcement discontinuities*. 2014, Purdue University.
14. Almeida, J.P., et al., *Influence of lap splices on the deformation capacity of rc walls. i: Database assembly, recent experimental data, and findings for model development.* ASCE J. Struct. Eng., 2017. **143**(12).
15. Pollalis, W.G., *Drift Capacity of Reinforced Concrete Walls with Lap Splices*. 2021: Purdue University Graduate School.
16. American Concrete Institute, *ACI 318-19: Building Code Requirements for Structural Concrete and Commentary*. 2019: Michigan, USA.
17. NZS3101:2006-A3, *Concrete Structures Standard Incorporating Amendment No. 1, 2, and 3.* 2017, Standards New Zealand: Wellington, New Zealand.
18. ATC, *FEMA 307: Evaluation of earthquake damaged concrete and masonry wall buildings*. 1998, Applied Technology Council Redwood City, CA.
19. Shah, P.P., *Seismic drift demands*. 2021, Purdue University.
20. *C5-1A: Part C - Detailed Seismic Assessment of Concrete Buildings C5-1A: Technical proposal to revisit the Engineering Assessment Guidelines*. 2018, Ministry of Buisness Innovation & Employment: Wellington, New Zealand.
21. *ACI 318-19 Building Code Requirements for Structural Concrete and Commentary*. 2019, Farmington, Hills, MI: American Concrete Institute.

22. Schuler, H., F. Meier, and B. Trost, *Influence of the tension shift effect on the force–displacement curve of reinforced concrete shear walls.* Engineering Structures, 2023. **274**: p. 115144.
23. Pollalis, W.G., C.S. Kerby, and S. Pujol, *On estimating the drift capacity of reinforced concrete walls with lap splices at their bases.* Bulletin of Earthquake Engineering, 2024(Special Issue: Modeling and Design of RC Structural Wall Systems.).

Appendix A – Methodology

This appendix summarizes the experimental program, including the test setup, specimen design, construction methods, and material properties.

Test Setup

Six walls were tested at the University of Canterbury's Structural Engineering Laboratory. A photograph of the test setup is provided in Figure 6. Walls had 270-mm wide and 2000-mm long rectangular cross sections and a clear height from top of foundation to centreline of application of lateral load of 6450 mm. The shear-span-to-wall-length aspect ratio of the walls was approximately 3.2.

Lateral load was applied by a pair of 1000kN actuators connected to a transfer beam. Lateral loading was displacement controlled, such that two cycles to each drift target of Table 1 were completed, where drift ratio is calculated as the lateral deflection at the centreline of application of lateral load divided by the 6450mm shear span. The wall was braced out-of-plane by pairs of square hollow sections at approximately one and two thirds of the wall height. Axial load was applied at the top of each wall by four centre-hole hydraulic jacks. Applied axial load was forced controlled within 5% of 1000kN for the duration of testing. At a section taken just above the top of foundation, the axial load ratio was approximately $0.07 * f_c' * A_g$ including applied axial load, wall self weight, and the weight of the test setup components. Tests were ended when walls lost either half of the peak lateral resistance or the ability to carry the applied axial load.

Table 1: Lateral loading history

Target Drift Ratio	Lateral Displacement (mm)	Number of Cycles
0.15%	9.7	2
0.20%	12.9	2
0.30%	19.4	2
0.40%	25.8	2
0.60%	38.7	2
0.80%	51.6	2
1.00%	64.5	2
1.25%	80.6	2
1.50%	96.8	2
2.00%	129	2
2.50%	161.3	2
3.00%	193.5	2
3.50%	225.8	2
4.00%	258	2

Wall Design

Nominal cross sections taken just above the top of foundation are illustrated in Figure 7. All reinforcement designs met or exceeded the strictest requirements of NZS 3101:2006 (A3) [17] for "ductile plastic regions" of doubly reinforced concrete walls.

Longitudinal boundary element reinforcement was arranged in three rows of two HD25 (25 mm) deformed bars. Web longitudinal reinforcement consisted of HD16 (16 mm) deformed bars spaced at approximately 230mm on each face. All lap splice lengths were 40 d_b, where d_b is the spliced bar diameter. Splices were designed using clause 8.6.3.3 of NZS 3101:2006 (A3), the calculations for "refined" development lengths in tension (see Appendix C). Lap splices were staggered by 20 d_b in walls W1, W2, W3, and W5. Clear cover to the transverse reinforcement was 1.0 d_b, and clear cover between spliced longitudinal bars was 1.6 d_b.

Table 2 describes the key differences between each of the six walls. Wall designs differed primarily by splice location, stagger pattern, and quantity of confining reinforcement. Figure 8 illustrates the lap splice locations in each wall. In W1, the lowest lap splice was in the exterior-most layer of bars in the boundary element and web, with splices staggered up towards the wall centreline. In W2 the lowest lap splice was located in the interior layer of bars in the boundary element and web, with splices staggered up towards the wall edge. W3 had staggered lap splices in the same pattern as W1. W4 had non-staggered lap splices all starting just above the top of foundation. W5 had staggered lap splices in a similar pattern as W2, but the spacing of the boundary element longitudinal bars was doubled (Figure 7). WC had no lap splices, instead mechanically coupling longitudinal bars just above the top of foundation.

Table 2: Wall design parameters

Wall	Splice Type	Lowest splice	Confined Boundary Element Length*	ρ_l	ρ_{tr}
W1	staggered laps	exterior	$0.14 * L_w$	3.9%	0.4%
W2	staggered laps	interior	$0.14 * L_w$	3.9%	0.4%
W3	staggered laps	exterior	$0.15 * L_w$	3.6%	1.1%
W4	non-staggered laps	n/a	$0.15 * L_w$	3.6%	1.1%
W5	staggered laps	interior	$0.23 * L_w$	2.6%	0.4%
WC	mechanical couplers	n/a	$0.14 * L_w$	3.9%	1.1%

*Confined Boundary Element Length refers to the largest confined length of a single boundary element in the full height of the splice region

L_w is the wall length (2000 mm)

ρ_l is the approximate boundary element longitudinal reinforcement ratio

ρ_{tr} is the approximate boundary element transverse reinforcement ratio

Boundary element confining reinforcement in W1, W2, and W5 consisted of 10mm diameter round bar hoops spaced at 150 mm and met the minimum requirement for NZS 3101 "ductile detailing" for confinement and anti-buckling. Boundary element confining reinforcement in W3, W4, and WC consisted of 12mm diameter round bar hoops spaced at 75 mm and was over twice the required quantity of transverse reinforcement to achieve NZS 3101 "ductile detailing". Web hoops in all walls consisted of 10mm diameter hoops spaced at 150 mm. Transverse reinforcement 135° hook locations were alternated up the wall height. Horizontal reinforcement for shear consisted of 10mm diameter deformed bars at 150mm in all walls, anchored with 90-degree hooks into the confined core of the boundary elements.

Mechanical couplers

Mechanical couplers were used to splice vertical reinforcement in Wall WC instead of lap splices. The couplers used were "Iron Man Bar-Coupler Mechanical Splice (IMBMS) Couplers for 25mm and 16mm reinforcement. Reinforcing bar ends to be spliced were threaded prior to delivery. Mechanical couplers were spun evenly onto the threads of each mechanically spliced bar, and a lock-nut wrench tightened on one end. Couplers were proven to be able to fracture reinforcement in monotonic and cyclic tensile tests of rebar samples.

Construction

Wall construction occurred in two stages: walls were cast on their side at a uniform thickness of 270 mm. The top portion of the walls was constructed at 6850mm high by 2000mm long. The base of the walls was 1250mm high by 4000mm long. The largest distance between top longitudinal bars and top of formwork in any of the six walls was approximately 220 mm, less than the 300 mm (12 in.) maximum distance before top-casting factors are applied in NZS 3101:2006 (A3) [17] and ACI318-19 [21]. There was no evidence in any of the six walls that top-casting effects reduced the bond strength of top cast lap splices.

After at least 14 days after the casting date, walls were tilted upright, and the 4000 mm-long bases were sandwiched between a pair of 780 mm-thick, precast reinforced-concrete blocks. 20 mm-wide gaps between wall bases and precast blocks were filled with shrinkage-compensated 40MPa grout, forming a foundation with friction planes either side of the wall base. Exposed faces of the wall base and precast blocks were roughened prior to grouting with ridges approximately five to ten millimetres in depth. Foundations had ducts perpendicular to the direction of lateral loading for the purpose of post-tensioning vertically (250kN at 40 locations) and horizontally (400kN at 16 locations) to prevent slip between foundation and floor.

After completing of testing a given wall, the grout faces bonding the precast foundation blocks to the wall base were split using hydraulic jacks, such that the wall could be disposed of. Any remaining grout was removed from the faces of the precast foundation blocks and the blocks were reused for the next test.

Material Properties

Test-day concrete properties are listed in Table 3. Parameters listed include f_c', the test-day compressive strength, f_t, the test-day split tensile strength, and E, the modulus of elasticity. Target concrete compressive strength was 30 MPa. Walls were cured under plastic sheeting and burlap, wetted twice daily. Curing duration varied from 3 to 14 days and was a function of the early strength of each concrete mix. Measured concrete compressive strengths were obtained from the mean test-day strength of three concrete cylinders, cast and cured under the same conditions as their respective test walls. Concrete cylinders were 200 mm by 100 mm.

The nominal grade of all reinforcement was AS/NZS 4671 Grade 500E. Each specimen was reinforced with steel from a single heat for each diameter reinforcing bar. Table 4 lists steel material properties for each steel heat of 25mm longitudinal steel, averaged from three monotonic tensile tests. The parameters listed include yield stresses (f_y), steel strain at onset of strain hardening (ε_{sh}), ultimate bar stress (f_u), and strain at ultimate bar stress (ε_u). The 25-mm diameter reinforcing steel used in all wall tests had well-defined yield plateaus.

Table 3: Concrete test-day mean measured material properties

Wall	f_c'	f_t		E
	MPa	MPa	$\sqrt{f_c'}$	GPa
W1	30.3	2.4	0.44	22.7
W2	29.3	2.4	0.44	24.6
W3	31.0	2.5	0.45	23.4
W4	32.8	2.6	0.45	25.5
W5	33.6	2.8	0.48	26.0
WC	33.2	2.9	0.50	27.1

Table 4: 25mm reinforcing steel mean measured material properties

Wall	d_b	f_y	f_u	ε_{sh}	ε_u
	mm	MPa	MPa	%	%
W1-W2	25	544	676	1.5	10.6
W3-W4	25	530	676	1.3	10
W5	25	534	673	1.5	10.3
WC	25	536	673	1.5	10.2

Figure 6: Test setup photograph

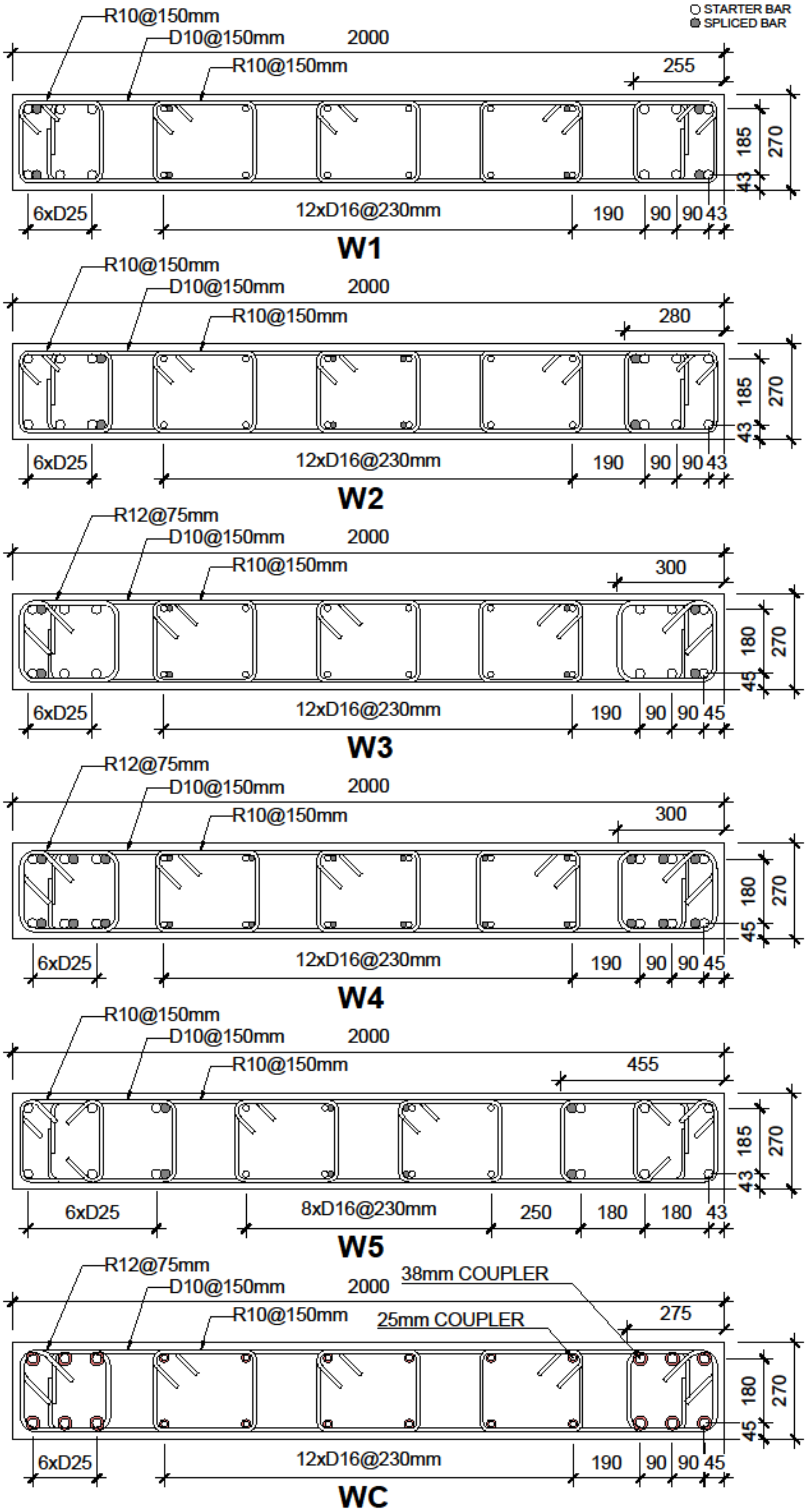

Figure 7: Wall cross sections at top of foundation

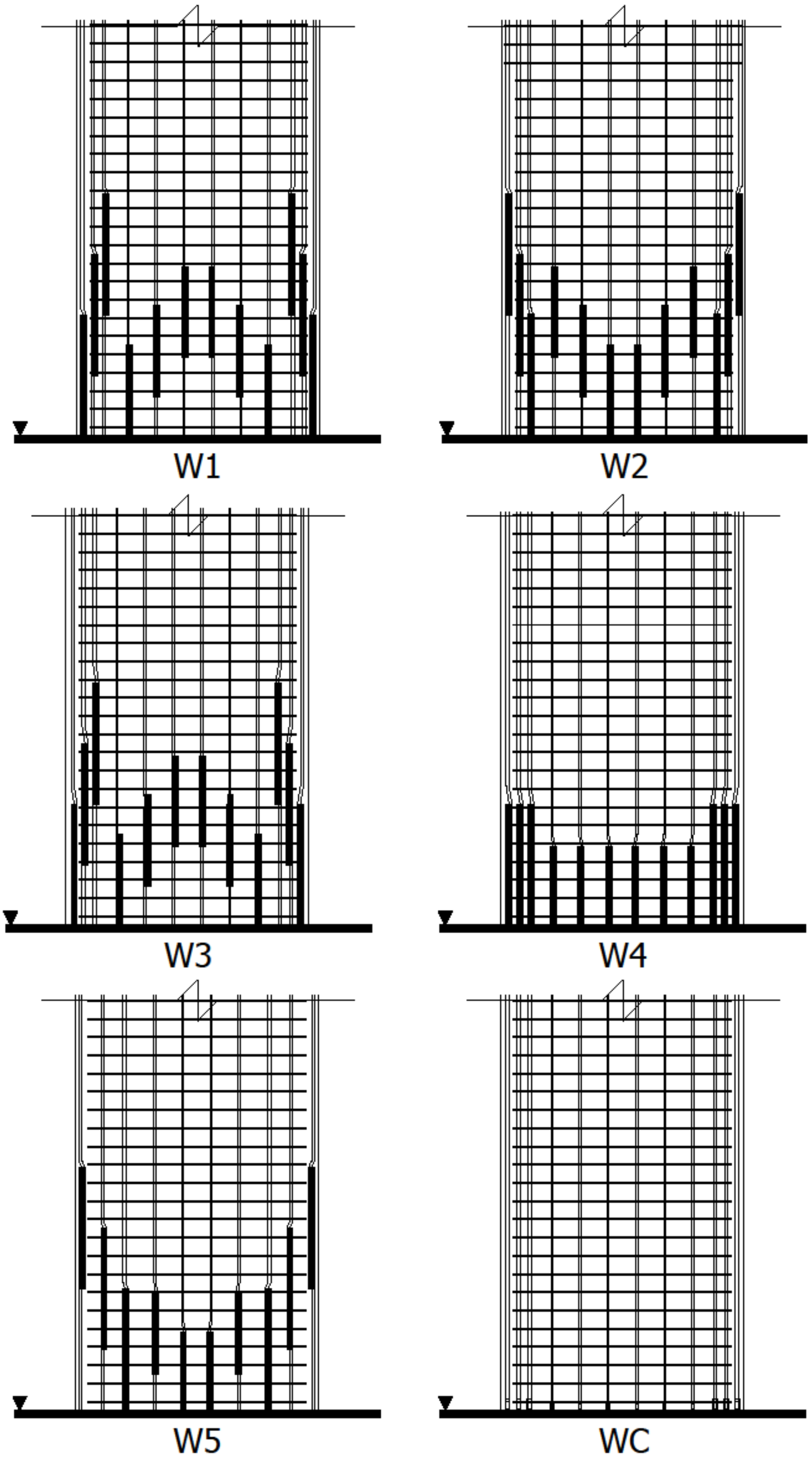

Figure 8: Lap splice layouts

Appendix B – Results

Lateral load vs drift ratio plots for each wall are presented in Figure 9. Photos of the front face of each wall after testing are presented in Figure 10. Table 5 summarizes the peak loads and drift ratios achieved during each test, as well as the drift ratio at first failure of the walls. Splice strengths were inferred from sectional analysis of the wall given the peak lateral load and section corresponding to the bottom of the lap splice which was observed to have failed first. Tension shift effects were accounted for in the sectional analysis via the method described by [22]. Drift ratio at first failure was defined at the drift when the first loss of lateral resistance occurred relative to the peak resistance previously achieved.

Table 5: Important loads and drift ratios during wall tests

Test Wall	Splice Type	Loading Direction	Peak Load	Splice Strength Inferred from Experiment	Drift Ratio at First Failure
			kN	MPa	%
W1	Staggered Laps	+	734	562	1.0
		-	-749	574	
W2	Staggered Laps	+	744	536	1.25
		-	-764	536	
W3	Staggered Laps	+	784	596	1.7
		-	-816	620	
W4	Non-Staggered Laps	+	816	620	2.3
		-	-853	641	
W5	Staggered Laps	+	712	578	2.1
		-	-746	594	
WC	Mechanical Coupler	+	797	n/a	3.5
		-	-840	n/a	

Damage Patterns and Failure Modes

In this section the development of damage during testing and the failure modes of the walls are described. The following statements are true of all the test walls.

1) Global yielding of the boundary elements occurred at approximately 0.7% drift.
2) Lap splices reached or exceeded reinforcement yield strength.
3) Tensile bond failure of lap splices was rapid if not near instantaneous.

Wall W1

Damage concentrated up the length of the lowest lap splices. Inelastic deformations concentrated at a single wide flexural crack just above the top of foundation. Splitting crack widths were measured at 2.0 mm near the ends and 0.75 mm in the middle of the lowest lap splices during the cycles immediately prior to bond failure occurring. The exterior-most lap splices, starting just above the top of the foundation, failed in bond during cycles to 1.0% drift. Concrete at the corners of the wall spalled along each splice length after bond failure. The middle layer of boundary element splices, starting 500 mm above the top of foundation, failed in bond during cycles to 2.0% drift and caused local spalling of concrete at the top end of the laps, 1500mm above the top of foundation (visible on the upper righthand side of Figure 10a).

Wall W2

Damage concentrated along the exterior-most boundary element lap splice, which started 1000mm above the top of foundation. Inelastic deformations concentrated at a single wide flexural crack just above the top of foundation, as observed during testing of W1. Bond failure of the exterior and middle layers of lap splices (starting 1000mm and 500mm above the top of foundation respectively) occurred during the cycles to 1.25% and 1.5% drift. Sectional analysis of W2 would suggest that the interior-most boundary element lap splices, starting 0mm above the top of foundation, should have failed prior to the exterior splices. It was concluded that the splices in W2 had varying bond strengths, likely due to differences in as-built concrete cover within the splice region. As splice strengths in W2 barely exceeded the reinforcing bar yield strength, small differences in bond strength could have resulted in a relatively large difference in splice strain capacity. Splitting cracks along the exterior splices were measured to be at least 2.0mm wide at splice ends and up to 1.0mm wide within the splice length prior during the cycles preceding bond failure. Splitting cracks were not exclusively vertical, but inclined and spanning both the exterior and middle splices, contributing to the failure of the middle layer of splices soon after the exterior-most splices.

Wall W3

The high boundary element transverse reinforcement ratio of Wall W3 ($\rho_{tr} = 1.1\%$) ensured lap splices had increased strength and strain capacity. As observed during testing of Walls W1 and W2, only a single wide flexural crack opened, located just above the top of the foundation. Splice failure of the exterior splice (starting 0mm above the top of foundation) occurred during cycles to 2.0% drift. Splitting cracks along the exterior splices were measured at 1.5mm wide near splice ends and approximately 0.5mm within the splice length prior to bond failure. After the first bond failure, concrete spalled along the length of the exterior splices and within the lowest 500mm of the wall. Inelastic deformations spread within the lowest 500mm of the wall (below the start of the middle lap splice) after failure of the exterior splice. The starter bars for all the boundary element bars and the exterior-most web bars buckled during cycles succeeding the bond failure of the exterior boundary element splices, contributing to the extensive spalling visible in Figure 10c. The middle boundary element lap splices failed in bond during the first cycles to 3.0% drift.

Wall W4

Inelastic flexural deformations concentrated at a single crack just above the foundation (as in W1, W2, and W3) but also above the 1000mm non-staggered splice region. The plasticity present above the splice region in W4 is visible in the spalling located at the top of the splice region in Figure 10d. The shorter splice region (relative to the 2000mm staggered splice regions of W1, W2, and W3) allowed plasticity above the lap splices of W4 and relatively decreased the strain demands on the lap splices, delaying tensile bond failure. The exterior and middle layers of lap splices failed during the first and second cycles to 2.5% drift respectively. Splitting cracks on the exterior lap splices were measured at 1.0-1.5mm wide near splice ends and 0.5-0.75mm wide within the splice length during the cycle immediately preceding bond failure.

Wall W5

Inelastic strains were observed at a single crack at the top of foundation but also within the boundary element below the start of the middle lap splice. The lowest splice (the interior 25mm bar) was sufficiently far into the wall length as to not restrain all inelastic deformations in the boundary element as had been observed in W2. Spalling began when the exterior and middle layers of boundary element bars buckled during cycles to 2.5% drift. The observed buckling length of individual bars was between 250mm and 300mm. The first observed tensile failure was the bond failure of the interior boundary element lap splices during cycles to 2.5% drift. Splitting cracks were measured no larger than 0.75mm near splice ends and 0.3-0.5mm within the splice length prior to bond failure of the interior splices, relatively smaller splitting crack widths than had been measured in W1 and W2 immediately preceding bond failure. Splitting cracks had exceeded widths of 1.5mm near the top end of the exterior splices (starting at 1000mm and finishing at 2000mm above the top of foundation), but the exterior splices did not fail in bond. Local spalling occurred at the top of the interior splices after bond failure, as is visible in Figure 10f. The exterior boundary element bars near the base of the wall fractured because of low-cycle fatigue during cycles to 3.0% drift.

Wall WC

Inelastic deformations were observed to be distributed within approximately 1750mm from the top of the foundation. Having no lap splices preventing distributed plasticity, the strains reached at a given strain in WC were relatively lower than in any other wall. The decreased strain demands also resulted in a slower strength gain after yield in WC relative to W3 or W4. Failure occurred when the western boundary element globally buckled during the second cycle to 3.5% drift and the wall lost axial load carrying capacity when loaded in the positive direction (Figure 11). The target axial load could not be reachieved after the boundary element instability developed. No failure was observed to have resulted from the use of mechanical couplers.

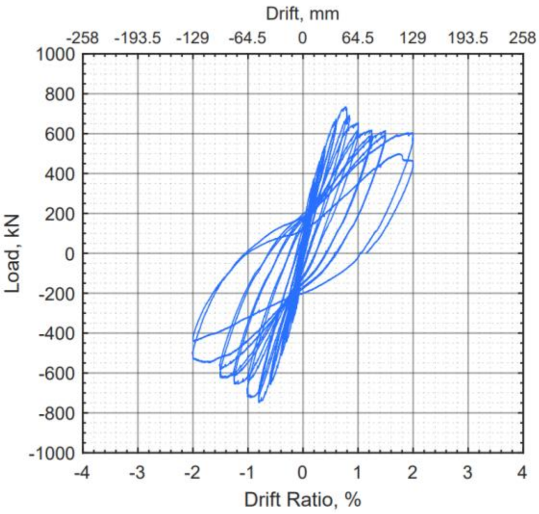

a) W1

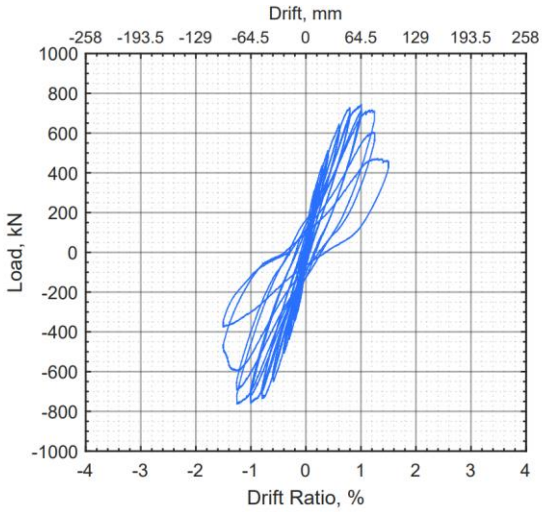

b) W2

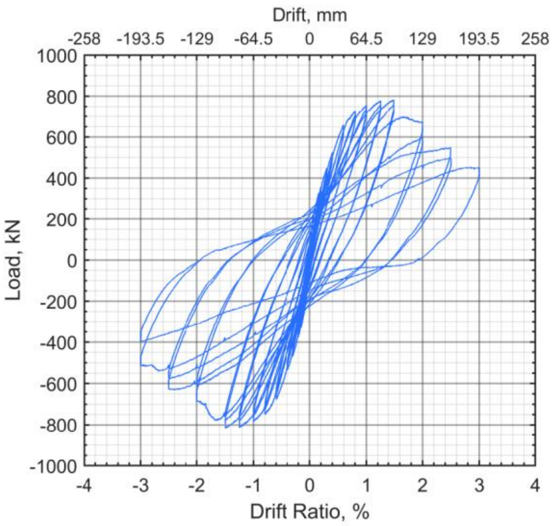

c) W3

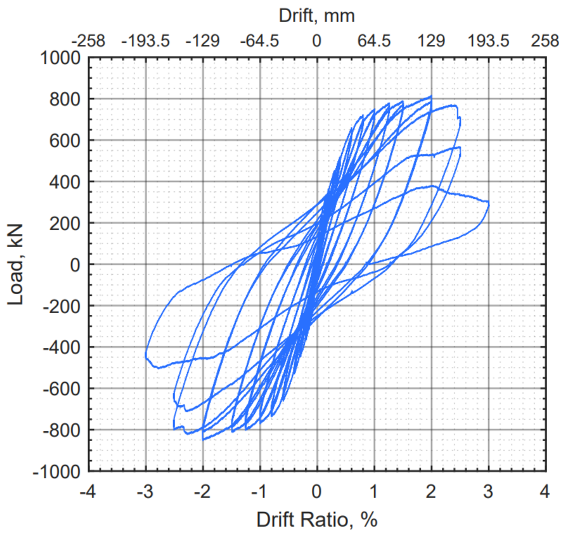

d) W4

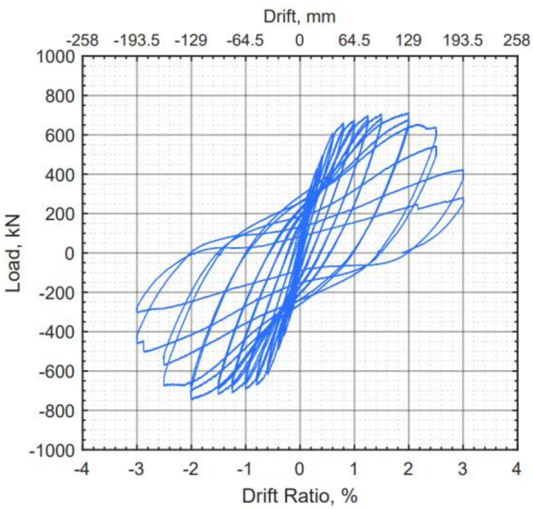

e) W5

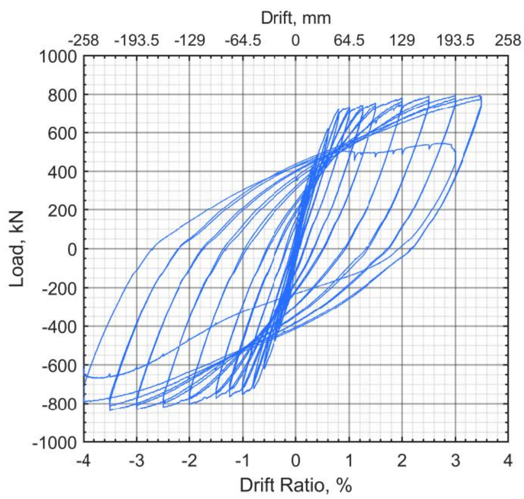

f) WC

Figure 9: Load versus drift ratio plots for all walls

a) W1

b) W2

c) W3

d) W4

e) W5

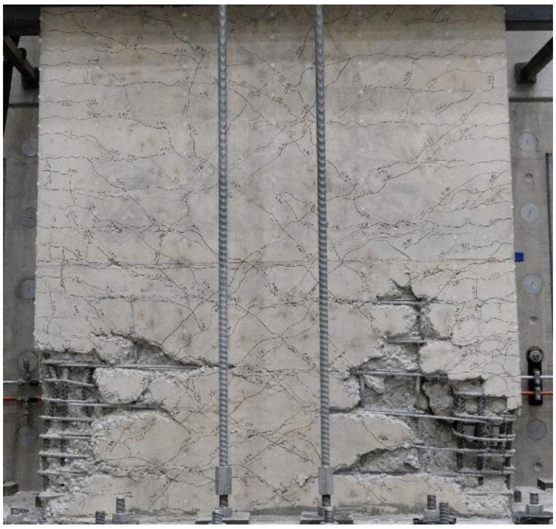

f) WC

Figure 10: Damage to front face of walls at conclusion of testing

Figure 11: Buckling of the western boundary element of WC at 3.5% drift

Appendix C – Modified calculation of design drift capacities

While the simple assumptions used to define the design drift capacity shown in Figure 5 (2.84%) are likely to be employed by practicing engineers, it is possible to produce more conservative design drift capacities for the six test walls using the methods currently in NZS 3101 [17]. The key assumption an engineer would need to make to produce Figure 5 would be that any lap splice longer in length than the code-defined development length can achieve both high stresses and high strains. An astute engineer who is familiar with lap splices might realize that assumption is unreasonable. This appendix shows an example of how design drift capacities for each of the six walls might be calculated by an engineer who chooses to consider lap splice strain capacity when estimating wall deformability. The methodology draws primarily on the text of NZS 3101:2006 (A3) [17], and uses simple mechanics to fill in any steps not explicitly covered in the standard.

Upper and lower bound design drift capacities were estimated for each of the five walls with lap splices. The calculation methods used are described in detail at the end of this appendix. Design drift capacities bounds were based on assumptions made in calculating lap splice strengths, determining lap splice strain capacities, selecting limiting concrete compressive strains, and sizing assumed plastic hinge lengths. Variable values used in calculating lower and upper design drift capacities are listed in Table 6 (lower) and Table 7 (upper). Where applicable, values were taken from as-built conditions to minimize error. Notes are included in the methodologies where alternate equations or values were used in the calculations for lower and upper bound design drift capacities.

The only difference between the lower and upper bound design drift capacities for the wall with mechanical couplers was the assumed plastic hinge length, as both calculations were limited by $K_{d,max}$ (defined below).

All equations in this appendix are reproduced and/or rearranged from NZS 3101:2006 (A3) [17]. Thus, all estimates of design drift capacity employ the plastic hinge analogy, which has been experimentally shown in this report to not be applicable to walls with lap splices (Figure 4). For those interested in methods to estimate drift capacity better representing the deformation mechanics of RC walls with lap splices, see [23].

Disclaimer

The bounds for design drift capacities produced in this appendix are illustrative of reasonable values a designer engineer using NZS 3101 [17] might produce, but do not represent all the values of design drift capacity that could be calculated. Changing any of the assumptions made in these calculations might produce vastly different results. The calculations presented in this appendix are representative only of the authors interpretation of NZS 3101 [17] and the authors understanding of the assumptions a practicing structural engineer might make.

Discussion of detailed design drift capacities

Experimental drift ratios at first failure are plotted with the lower and upper design drift capacity bounds in Figure 12.

Considering lap splice strain capacities improved the estimates of design drift capacities for all the walls with lap splices, but not enough to make the estimates conservative in nature. Only Wall WC, without any lap splices, exceeded both the lower and upper bound design drift capacities, and is thus ensured to be conservatively designed. The experimental drift at failure of Wall W4 is approximately equal to the average of the lower and upper bound design drift capacities, meaning that non-conservative design of W4 is reasonably possible. Non-conservative design of Walls W2 and W5 is likely, as experimental drifts at first failure are close to the lower bound design drift capacities for each wall. For Walls W1 and W3, the experimental drifts at first failure are lower than even the lower bound design drift capacities, such that non-conservative design is certain. The lower bound design drift capacity of Wall W3 is more than 1.5 times larger than the experimental drift at first failure, suggesting that the largest discrepancy of deformability between design expectation and reality may be present for walls with staggered lap splices having high strain capacities.

The conclusions that can be drawn from Figure 12 are the same as were drawn Figure 5, that current design practice overestimates the deformability of walls with lap splices. It has been shown for walls with staggered lap splices, even an engineer attempting to make conservative assumptions would be likely to calculate a non-conservative design drift capacity when using [17]. This reinforces the conclusions that 1) staggered lap splices reduce the deformation of RC walls relative to walls with no lap splices 2) the deformation capacity of walls with lap splices designed under current and previous iterations of the New Zealand RC standards should be reassessed.

Table 6: Values for lower bound calculations of NZS 3101:2006 (A3) design drift limits

Wall	$f_{s,3101}$	ε_{max}	c_m	d_{tr}	s	d	l_p	φ_p	φ_y	K_d	Design drift capacity
	MPa	%	mm	mm	mm	mm	mm	1/m	1/m		%
W1	557	1.7	31	10	150	1945	967.5	0.0103	0.0021	5	1.02
W2	548	1.5	30	10	150	1765	967.5	0.0102	0.0021	5	1.02
W3	646	4.9	31	12	75	1943	967.5	0.0268	0.0021	13	2.64
W4	626	3.7	35	12	75	1943	967.5	0.0206	0.0021	10	2.03
W5	587	2.7	34	10	150	1585	967.5	0.0189	0.0021	9	1.83
WC	x	x	33	10	75	1943	967.5	x	0.0021	14	2.84

Table 7: Values for upper bound calculations of NZS 3101:2006:A3 design drift limits

Wall	$f_{s,3101}$	ε_{max}	c_m	d_{tr}	s	d	l_p	φ_p	φ_y	K_d	Design drift capacity
	MPa	%	mm	mm	mm	mm	mm	1/m	1/m		%
W1	606	3.1	31	10	150	1945	1000	0.0214	0.0021	10	2.10
W2	596	2.7	30	10	150	1765	1000	0.0213	0.0021	10	2.10
W3	676	10.0	31	12	75	1943	1000	0.0575	0.0021	14	2.94
W4	626	3.9	35	12	75	1943	1000	0.0256	0.0021	12	2.52
W5	638	4.6	34	10	150	1585	1000	0.0360	0.0021	14	2.94
WC	x	x	33	10	75	1943	1000	x	0.0021	14	2.94

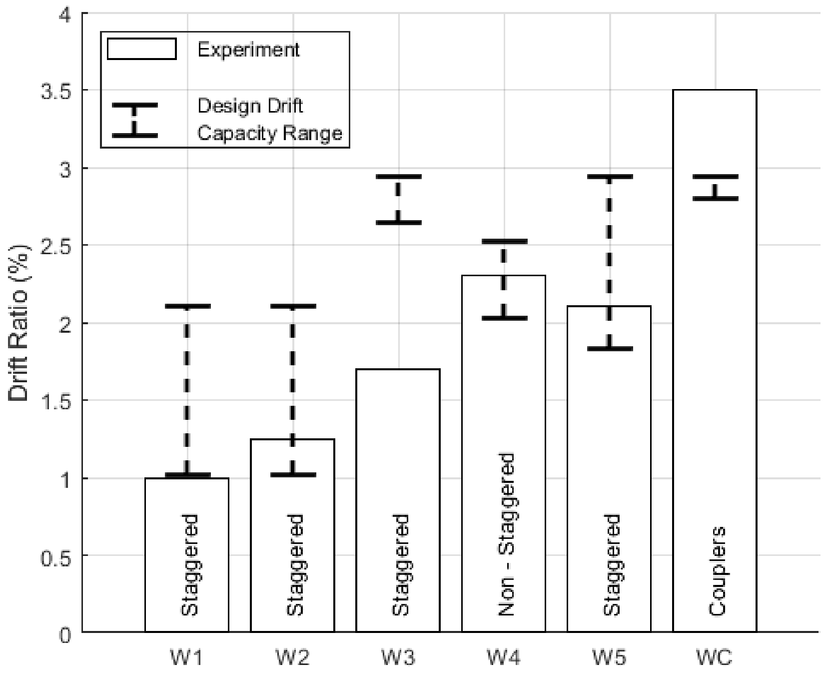

Figure 12: Experimental drift ratios at first failure versus a plausible range of design drift capacities according to NZS 3101:2006 (A3) [17]

Method for calculating design drift capacities of test walls with lap splices:

1) Lap splice strength ($f_{s,3101}$) was estimated using Eq. 1

$$f_{s,3101} = l_d * \frac{\alpha_c * \alpha_d}{\alpha_b} * \sqrt{f_c'} * \frac{1}{0.5 * d_b} \leq f_{ult} \qquad \text{(Eq. 1)}$$

where

l_d	is the splice length, taken as 1000mm for all splices in this report
α_b	is a reinforcement quantity factor, taken as unity in this report
α_c	$= 1 + 0.5 * \left(\frac{c_m}{d_b} - 1.5\right)$, a concrete cover factor limited to $1.0 \leq \alpha_c \leq 1.5$
c_m	is the lesser of the concrete cover or the clear distance between bars
α_d	$= 1 + \sqrt{\left(\frac{A_{tr}}{s}\right)\left(\frac{f_{yt}}{80*n*d_b}\right)}$, a transverse reinforcement factor limited to $1.0 \leq \alpha_d \leq 1.5$
A_{tr}	is the area of one leg of the transverse reinforcement confining the lap splice
s	is the spacing of the transverse reinforcement
n	is the number of lap splices being developed at the critical section taken as 2 for LOWER BOUND and 1 for UPPER BOUND staggered splice strengths taken as 3 for both LOWER BOUND and UPPER BOUND non-staggered splice strengths
f_{yt}	is the yield stress of the transverse reinforcement, taken as 540 MPa in this report
f_c'	is the test-day concrete strength as reported in Table 3
d_b	is the spliced bar diameter
f_{ult}	is the ultimate stress of the reinforcement

2) Lap splice strain capacities (ε_{max}) were estimated using the calculated value of $f_{s,3101}$ from Eq. 2 and stress-strain profiles from monotonic tensile tests of reinforcement samples used in the construction of the walls

3) The plastic hinge rotation at first yield (φ_y) was estimated using Eq. 2

$$\varphi_y = \frac{2 * 425\ MPa}{E_s * L_w} \qquad \text{(Eq. 2)}$$

where

E_s	is the elastic modulus of steel, taken as 200 GPa
L_w	is the length of the wall, taken as 2000 mm

4) The plastic hinge rotation at the ultimate limit state (φ_p) was estimated using Eq. 3a for LOWER BOUND and Eq. 3b for UPPER BOUND design drift capacity calculations

$$\varphi_p = \frac{0.003 + \varepsilon_{max}}{d} = K_d * \varphi_y \leq K_{d,max} * \varphi_y \qquad \text{(Eq. 3a)}$$

$$\varphi_p = \frac{0.01 + \varepsilon_{max}}{d - c_m} = K_d * \varphi_y \leq K_{d,max} * \varphi_y \qquad \text{(Eq. 3b)}$$

where

$0.003, 0.01$	are limiting concrete strains, assuming unconfined and confined concrete respectively
d	is distance from the extreme compression fibre to the centroid of the lowest boundary element splice
K_d	is the ratio φ_p / φ_y
$K_{d,max}$	is taken as 14, for doubly reinforced walls with ductile detailing according to NZS 3101:2006 (A3) Table 2.4.

5) Plastic hinge length (l_p) was estimated using Eq. 4a for LOWER BOUND and Eq. 2b for UPPER BOUND design drift capacity calculations

$$l_p = 0.15 * a \qquad \text{(Eq. 4a)}$$

$$l_p = 0.5 * L_w \qquad \text{(Eq. 4b)}$$

where

a	is the shear span, taken as 6.45 meters

6) The design drift capacity was estimated using Eq. 5

$$Design\ drift\ capacity\ = \varphi_p * l_p \qquad \text{(Eq. 5)}$$

Method for calculating design drift capacities of Wall WC, with mechanical couplers:

1) The plastic hinge rotation at first yield (φ_y) was estimated using Eq. 2.
2) Because no lap splices were present, it was assumed that the mechanical couplers could fracture the longitudinal reinforcement. K_d was set equal to $K_{d,max}$ at a value of 14
3) Plastic hinge length (l_p) was calculated using Eq. 4a or 4b.
4) The design drift capacity was estimated using Eq. 5.

Method for calculating the design drift capacity of Figure 5 (2.84%):

1) The plastic hinge rotation at first yield (φ_y) was estimated using Eq. 2.
2) Splice lengths were confirmed to exceed the refined development lengths in tension as defined in NZS 3101 Section 8.6.3.3.
3) Detailing of all test walls were confirmed to satisfy the additional design requirements for walls designed for ductility in earthquakes, as defined in NZS 3101:2006 (A3) Section 11.4. K_d was assumed equal to $K_{d,max}$ at a value of 14.
4) Plastic hinge length (l_p) was calculated as the minimum of Eq. 4a and 4b.
5) The design drift capacity was estimated using Eq. 5.